University of Kurdistan
Dept. of Electrical Engineering
Smart/Micro Grids Research Center
smgrc.uok.ac.ir

Robust Frequency Control of Microgrids Using an Extended Virtual Synchronous Generator

Abdolwahhab Fathi, Qobad Shafiee, and Hassan Bevrani

Published (to be published) in: ***IEEE Transactions on Power Systems***

(Expected) publication date: **2018**

Citation format for published version:

A. Fathi, Q. Shafiee, and H. Bevrani ‘‘Robust Frequency Control of Microgrids Using an Extended Virtual Synchronous Generator,’’ *IEEE Transactions on Power Systems,* vol.x, no. x, pp. xx-xx, 2018.

Robust Frequency Control of Microgrids Using an Extended Virtual Synchronous Generator

Abdolwahhab Fathi, *Student Member, IEEE,* Qobad Shafiee, *Senior Member, IEEE,* Hassan Bevrani, *Senior Member, IEEE*

***Abstract*— Integration of inverter-interfaced distributed generators (DGs) via microgrids into traditional power systems reduces the total inertia and damping properties, while increasing uncertainty and sensitivity to the fault in the system. The concept of the virtual synchronous generator (VSG) has been recently introduced in the literature as a solution which mimics the behavior of conventional synchronous generators in large power systems. Parameters of the VSGs are normally determined comparing the conventional synchronous generators. This paper introduces an extended VSG (EVSG) for microgrids by combining the concept of virtual rotor, virtual primary and virtual secondary control as a virtual controller to stabilize/regulate the system frequency. An H_∞ robust control method is proposed for robust\optimal tuning of the virtual parameters. The effectiveness of the proposed control methodology is verified via a microgrid test bench.**

***Index Terms*— Frequency control, microgrids, robust control, virtual controller, virtual inertia, virtual synchronous generator.**

I. INTRODUCTION

RECENTLY, integration of renewable energy sources (RESs) into the traditional power systems is rapidly growing. The future plans address great and important purposes of using RESs all over the world. These sources and distributed generators (DGs) decentralize the generation of bulk power plants while adding more fluctuations and disturbances (due to natural changes and uncertainties in RESs) to the systems. Microgrid (MG), as a new concept, facilitates the integration of RESs\DGs into the distribution systems. Taking the idea from conventional power systems, a hierarchical control structure (i.e., *primary*, *secondary*, *central/emergency*, and *global* control levels) has been introduced for these small-scale power grids. This hierarchy provides more flexibility in using intelligent, optimal, robust and other advanced control techniques in MGs. While the upper control loops require communication to provide a good performance, the primary level, e.g., droop control, does not rely on communication and it is implemented in a decentralized manner [1]–[4]. Among the advanced control techniques, robust control methods, e.g., H_∞, μ-synthesis, and mixed H_2/H_∞, have recently received much attention in the MG applications [5]–[8]. Considering model uncertainty during the synthesis procedure is the great advantage of the linear robust control techniques. However, the order of designed state feedback controllers is normally bigger than the order of the controlled system.

In conventional power systems, the synchronous generators (SGs) provide inertia (due to rotating a heavy mass) and damping (due to mechanical friction and electrical losses in the stator, field, and damper windings) properties for the system [3]. These properties include an initial and intrinsic potential of the system that opposes changes against faults and disturbances. High penetration of the inverter-interfaced DGs/RESs reduces total inertia and damping of the conventional bulk power systems (e.g. 70% reduction in inertia constant is predicted in the period of 2014 and 2034, due to increases of the number of RESs [9]). Once inertia constant is reduced due to the above mentioned reasons, the rate of frequency changes is increased, and may load-shedding relays be activated even for small imbalances. As a result, the system becomes more sensitive to the faults/disturbances and its stability margin is reduced.

While integration of inverter-interfaced systems to the existing electricity grid is rapidly growing, most of the control methods and solutions introduced in the literature for these systems, e.g., conventional droop control, provide barely any inertia/damping support for the grid. To cope with this problem, the concept of virtual synchronous machine/ generator (VSM/VSG) has been presented recently [10], [11]. In fact, VSG mimics the behavior of conventional synchronous generators (SGs). This concept has been also introduced under the name of virtual inertia (VI) [3]. VSGs basically add some inertia to the system virtually and accordingly improve the power/micro grid's stability and performance. Since inertia response is the result of rotating heavy mass and it is proportional to the rotor speed, the VSG concept can directly improve the frequency response. A comprehensive survey on VSG and the existing topologies are given in [3], [12], and modeling of such a concept has been studied in some recent works, e.g., [13], [14]. Improving grid stability [1], [11], and smart/micro grids frequency response [15]-[17], as well as oscillation damping of DGs [1], [18], [19] have been introduced as the main applications of VSGs.

Proper performance of a VSG, which depends on its objective, is guaranteed via choosing appropriate values for its parameters, i.e., inertia constant and damping value. These parameters are conventionally determined via comparing the virtual and the real SGs. Recently, a few research works have introduced advanced control methods to determine the VSG parameters [17], [20]. In [17], the virtual inertia constant and virtual damping factor are optimized using particle swarm optimization (PSO) techniques to minimize the frequency and voltage deviation. A fuzzy-logic based method is proposed in [20] to define the virtual inertia constant. In [1], integration of

The authors are with the Smart/Micro Grids Research Center, University of Kurdistan, Sanandaj 66177-15175, Kurdistan, Iran. (e-mails: ab.fathi@eng.uok.ac.ir, q.shafiee@uok.ac.ir, bevrani@uok..ac.ir)

DGs to the grid has been presented under the concept of VSG with adoptive moment inertia.

Although advanced control methods have been utilized in these works to infinitely tune virtual parameters, they do not consider system uncertainties and disturbances which are very important in low inertia smart/micro grids. Yet, to the best of the author's knowledge, no robust control-based approach exists for the VSG concepts assuring system uncertainties.

Considering the essentials of CERTS regulation methods [28], this paper introduces the concept of *virtual inerti*a for frequency control of MGs via an extended VSG (EVSG). The proposed EVSG controller is applied to the inverter-based DGs as a *virtual controller* in the MG to support the frequency control and enhancing inertia response. The salient features of the proposed solution are briefly outlined as follows

- A virtual controller is proposed which mimics the inertia, damping property and frequency control loops characteristics of conventional SGs to be used by inverter-based DGs and contribute in grid frequency regulation. The controller combines the concept of a virtual rotor as well as virtual primary and secondary controllers used in the SGs. It compensates the inertia reduction in the power system as the results of adding non-inertia sources, e.g., RESs.
- An H_∞ robust control is proposed for the robust/optimal tuning of the virtual parameters. Unlike the existing works, the proposed solution can easily address inherent fluctuations and uncertainties in RESs. The designed robust compensator is correlated with the virtual controller using a simple synthesis procedure.
- Using the proposed virtual controller, required inertia is provided for the system to achieve a satisfactory frequency regulation under severe disturbances and system uncertainties.
- The proposed virtual controller structure inherits both properties of inertia response of real SGs and fast dynamics of power electronic interfaces, giving a high flexibility in designing procedure.

The rest of this paper is organized as follows. Section II describes a brief review on frequency control and VSG concept for inverter-based systems. In Section III, an MG test system is introduced. The H_∞ robust control for the MG system is designed based on its frequency response model, in Section IV. In section V, a new H_∞ robust control method is proposed for tuning the virtual parameters. Simulation results in MATLAB SimPowerSystems (SPS) toolbox is presented in Section VI. Section VIII concludes the paper.

II. Virtual Frequency Controller

Grid frequency stability is a balance criterion between generations and loads. In modern power grids, lack of inertia of inverter-interfaced DGs increases the rate of frequency change [1]. The VSG concept has drawn lots of attention to cope with this challenge, recently. This section aims to demonstrate background on frequency control issue and the VSG concept.

A. Frequency Control

In SGs, the relation between frequency deviation, generated active power, and load is expressed by a well-known swing equation (in Laplace domain) as [3]

$$\Delta P_m(s) - \Delta P_l(s) = 2H\,s\,\Delta f(\mathrm{s}) + D\,\Delta f(\mathrm{s}) \tag{1}$$

where Δf, ΔP_m, ΔP_l, H, and D, are frequency deviation, mechanical power change, load change, inertia constant, and load damping coefficient, respectively. Once H and/or D decrease (increase), the rate of frequency deviation and frequency deviation are increased (decreased). In smart/micro grids, however, the damping factor, D, is a small value while the total inertia constant, H, changes mainly depending on the number of DGs in the system. In such systems, the relation between DG's inertia constant (H_{DG}) and system's inertia constant (H_{sys}) is expressed as [21]

$$H_{sys} = \sum_i H_{DGi} \times \frac{S_{DGi}}{S_{sys}} \tag{2}$$

where S_{sys} and S_{DG} are nominal system's power and nominal DG's power, respectively. Therefore, by increasing the penetration and proportion of none/less-inertia DGs in the system, the H_{sys} is decreased.

In conventional power grids, network frequency generated by rotational mass is controlled in hierarchical levels. The stored kinetic energy of rotor is the first prevention against generation and loads imbalances. The primary and secondary control loops in most SGs, are used to restore the frequency deviation. Therefore, in conventional SGs, the frequency is controlled via two basic control loops:

- Primary control (governor natural response) loop, which clearly realizes the impact of rotating heavy mass (rotor) on the rate of frequency changes (inertia and damping properties)
- Secondary control loop, which is usually performed by an integral or proportional-integral (PI) controller.

Primary loop provides a local and automatic frequency control by adjusting the speed governors in the time frame of seconds after a disturbance. Secondary loop initializes a centralized frequency control task using the considered spinning reserve to restore frequency deviation, which is activated in the time frame of few seconds to minutes after a disturbance [3]. The aim of this paper is to emulate these two control loops together with the inertia and damping properties for the inverter-based DGs, virtually.

B. Inverter Frequency Model

The inverter is a power electronics interface that converts a dc voltage to an ac voltage. It can follow a reference signal by controlling the IGBT gates (e.g. using PWM method). Generally, the inverters have two separate operation modes, acting as a current source or as a voltage source [22]. The current and voltage equations of output filter (which convert a square inverter-output voltage to a sinusoidal form) are used in the modeling of inverter-based DGs. However, traditional modeling for inverters presents a first-order element (with

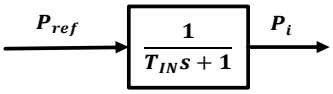

Fig. 1. Frequency response model for an inverter.

filter time constant) in the s-domain [23]. Given the value of line/filter parameters, the output voltage and frequency, as well as real and reactive powers of the inverter can be controlled using local feedbacks applied to the inverter [4], [23]. Therefore, inverters can follow reference power with a small time constant (T_{IN}), and, they can be modeled as a first-order transfer function, suitable for frequency analysis, as shown in Fig. 1. T_{IN} is the time constant that inverter can change input power to a regular voltage and frequency such that $4T_{IN}$ is considered as settling time of inverter. As a result, an inverter can be considered as an SG with a small time constant and none inertia response.

C. Virtual Rotor

According to the given swing equation in (1), for a specified frequency deviation, the amount of power that a source must compensate is obtained. Thus, the power reference (P_{ref}) for an inverter, e.g. inverter *i*, can be expressed as

$$P_{ref} = -(H_i s + D_i)\Delta f \tag{3}$$

The negative sign in (3) shows negative feedback. In this paper, H_i with D_i are considered as *virtual rotor* parameters.

D. Virtual Primary and Secondary Control

In conventional power systems, SGs are grid-forming units which have the task to provide a stable operating point, i.e., a synchronous frequency and a certain voltage level at all the buses in the network [21]. In inverter-based systems (e.g., inverter-intensive ac MGs), this capability is provided by voltage-source inverters (VSIs) [24]. The concept of droop control is often used in power systems to maintain the desired system frequency by adjusting the rotational speed of SGs. This control strategy allows parallel generators operation to achieve power sharing. Inspired by this concept, droop mechanism was extended to parallel-connected inverters [25], and later for MGs [2], [24].

The concept of *secondary control*, also known as load-frequency control (LFC), as the main block of automatic generation control (AGC), has been used in large power systems to address the steady-state frequency drift caused by the droop mechanisms. It is conventionally implemented via a slow, centralized PI controller with low bandwidth communication [3]. This concept has been also utilized for frequency regulation of MGs.

Combining the primary and secondary control loops, one can obtain a PI controller expressed as

$$\Delta P_{PI} = -(\frac{1}{R_i} + \frac{K_i}{s})\Delta f \tag{4}$$

where R_i and K_i are virtual droop characteristics and virtual secondary integrator gain, respectively.

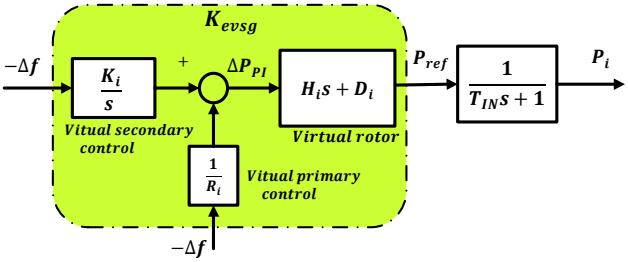

Fig. 2. Virtual controller in details.

E. Extended VSG

Combining the *virtual rotor* and the *virtual primary and secondary* controllers, an *extended virtual synchronous generator* (EVSG) is obtained as a virtual controller (K_{evsg})

$$K_{evsg} = \frac{(H_i s + D_i)(\frac{1}{R_i}s + K_i)}{s(10^{-6} \times s + 1)} \tag{5}$$

where H_i, D_i, R_i and K_i are *virtual parameters*. A remote pole is added to the controller which does not affect the controller in the operating frequency range but to ensure the system is causal. The designed controller can be now applied to the inverter-based DGs. The power signal reference for the inverter and virtual controller are shown in Fig. 2. Using the virtual controller, K_{evsg}, inverter-based DGs behave like SGs participated in frequency regulation.

III. Case Study

A MG test system is considered to design the proposed virtual controller and to study stability analysis. The test system consists of conventional diesel engine generator (DEG), photovoltaic (PV) systems, wind turbine generator (WTG), fuel cell system (FCs), battery energy storage system (BESS), and flywheel energy storage system (FESS). The components are connected to the MG by power electronic interfaces, i.e., inverters. Inverters are used for synchronization with ac sources, i.e., DEG, and to convert the output of dc sources like PVs, FC, and energy storage devices. Although, a wide variety of generation sources are considered in the test system, one can simply reduce the complexity by removing some of the sources. Moreover, since control structure for inverter-based DGs (e.g. FC, FESS, and BESS) is similar, they can be replaced by ideal sources.

In the case study, the PV_2 system equipped with storage system is added to evaluate the performance of the proposed EVSG. More details about the case study e.g., DGs size and loads is given in section VI. A simplified frequency model for this case study (sufficient for frequency analysis) is shown in Fig. 3, and the electrical parameters of the system are listed in Table I. For the sake of saving space, we only provide a brief discussion about the modeling. Interested readers can find detailed information in [26].

A PI controller is utilized for secondary control of the DEG, and accordingly regulation of the system frequency (see Fig. 3). Due to fluctuation and uncertainty in the MG generation and load, as well as less inertia of the power electronic-based

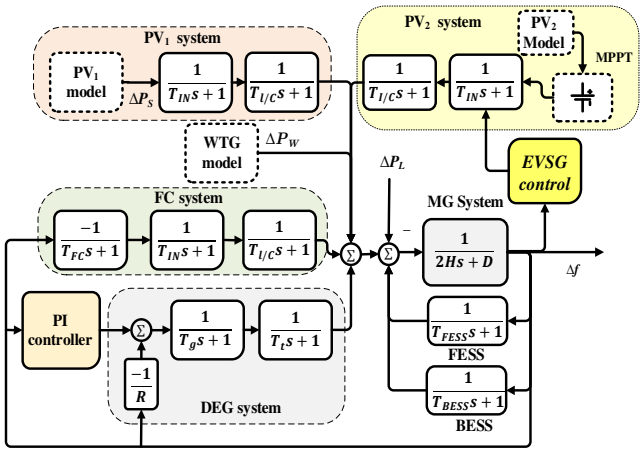

Fig. 3. Frequency response model of the MG test system.

TABLE I
THE ELECTRICAL PARAMETERS OF THE MG SYSTEM IN (FIG. 3)

Parameter	Value	Parameter	Value
D (pu/Hz)	0.015	T_g (s)	0.08
$2H$ (pu s)	0.1667	T_t (s)	0.4
T_{FESS} (s)	0.1	$T_{I/C}$ (s)	0.004
T_{BESS} (s)	0.1	T_{IN} (s)	0.04
T_{FC} (s)	0.26	R (Hz/pu)	3

DGs, the PI controller is not able to provide a reliable and desirable performance in a wide range of operating conditions (see Fig. 9). To cope with this issue, the PV_2 is used as an additional regulation source controlled by the designed EVSG controller. H_∞ robust control is applied for robust tuning of the EVSG's virtual parameters, improving the performance of the proposed controller.

IV. H_∞ ROBUST CONTROL

In this section, H_∞ robust control theorem is used to determine the optimal EVSG parameters (5) by designing of an equivalent robust controller (K_{H_∞}) for the MG test system in Fig. 3. The designing procedure of the robust controller is provided in the following subsections. Interested readers can find detailed information about linear robust control methods (H_∞, H_2, mixed H_2/H_∞, μ, etc.) in [3], [27].

A. Uncertainty Modeling

For the MG system in this study, H and D are considered as uncertain parameters (with ±90% changes). This uncertainty is extracted from the system in the form of structured uncertainty and arranged in a standard configuration of upper linear fractional transformation (LFT) as shown in Fig. 4, which depicted as Δ block.

B. Performance Consideration

The main goal of the frequency controller is to eliminate the frequency deviation, and, accordingly improving the system frequency stability. In this study, variations in wind speed (ΔP_W), solar radiation (ΔP_S), and load profile (ΔP_L) are considered as main sources of disturbances.

With above performance consideration, the whole system can be presented as Fig. 4. In this figure, G is the open loop MG test system, $pert_{in}$, $pert_{out}$, w, z, u and $-y$ are uncertainty block inputs, uncertainty block outputs,

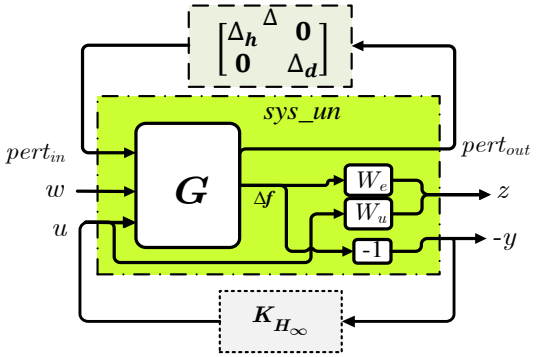

Fig. 4. Standard structure of case study MG for H_∞ synthesis with uncertain block.

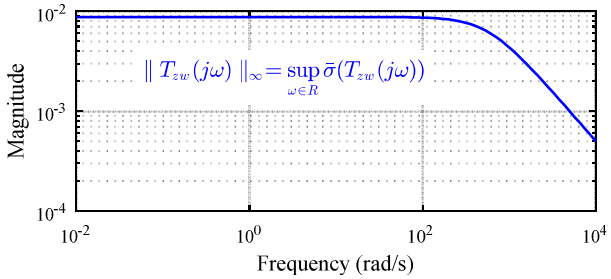

Fig. 5. Closed-Loop nominal performance of the control system.

disturbance signals, controlled output signals, control action signal and controller input, respectively. W_e and W_u are weighting functions that shaped and normalized the controlled output and control signals. The effects of these weighting functions in controller design are essential. It should be noted that there exists no analytical method to determine the weighting functions optimally. A trade-off is normally made among several performance requirements. Here, W_e affects the frequency deviation performance while W_u adjusts the control efforts. In [4], a suitable method is proposed to determine the weighting functions. In this study, the weighting functions are selected as following

$$W_e = \frac{0.005\,s^3 + 0.05\,s^2 + 50\,s + 125}{s^3 + 100\,s^2 + 300\,s + 1} \tag{6}$$

$$W_u = \frac{5\,s + 50}{s^2 + 2000\,s + 1.7\times10^4} \tag{7}$$

C. Optimal H_∞ Controller Design

The H_∞ control as an optimization control problem finds a feasible robust controller to minimize the ∞-norm of the T_{zw}, where T_{zw} is the transfer function from disturbance signals (w) to the controlled output signals (z) in the nominal closed-loop system. Since there exists no analytic method to solve this optimization problem, one can find a stabilizing controller such that the ∞-norm of T_{zw} satisfies the following condition.

$$\left\| T_{zw}(s) \right\|_\infty \le 1\,. \tag{8}$$

Using the robust control toolbox commands in MATLAB, the robust controller (K_{H_∞}) is obtained, whose order is 22.

D. Nominal Stability and Performance

The nominal stability (NS) is satisfied because the closed-loop system T_{zw} is internally stable for the designed K_{H_∞}. For evaluating the nominal performance (NP), the controller must satisfy the performance criterion for all frequencies as

$$\left\|T_{zw}(s)\right\|_\infty = \sup_{w\in R}\bar{\delta}\left(T_{zw}(jw)\right) \le 1 \tag{9}$$

Fig. 5 shows that the inequality of (9) is satisfied and is always less than one. Thus, the closed-loop system successfully reduces the influence of the disturbance, and the required performance is well achieved.

E. Closed-Loop Robust Stability and Performance

For the structured uncertainty, there exist two theorems for robust stability (RS) and robust performance (RP) based on *structured singular value* (μ)-synthesis methodology. The RS and RP are satisfied for the closed-loop system if and only if the closed-loop system is internally stable and satisfy the performance criterion, respectively, for all possible plants in the presence of uncertainty.

- Robust stability:
  Consider $M-\Delta$ configuration in Fig. 6(a). Assume

$$\Delta^* = \left\{\Delta(\cdot)\in RH_\infty, \Delta(s_0)\in\Delta^*, s_0 \in \not\emptyset, \mathrm{Re}(s_0)\ge 0\right\}, \tag{10}$$

$$\mathrm{M} = \begin{bmatrix} M_{11} & M_{12} \\ M_{21} & M_{22} \end{bmatrix} \tag{11}$$

where $M = F_L(G,K)$ is the system that contains the designed controller, and Δ is uncertainty block that expressed in general form as

$$\Delta = \left\{diag\left[\delta_1 I_{r1},\ldots,\delta_k I_{rk},\Delta_1,\ldots,\Delta_f\right], \delta_i \epsilon C, \Delta_j \epsilon C^{k_i\times k_j}\right\} \tag{12}$$

The closed loop of system for all $\Delta\in\Delta^*$ and $\left\|\Delta\right\|_\infty \le 1$ is internally stable if and only if the nominal system be stable and

$$\sup_{w\in R}\ \mu_\Delta\left(M_{11}\right) \le 1 \tag{13}$$

- Robust performance:
  Consider $M-\Delta_T$ configuration in Fig. 6(b). Let us assume

$$\Delta_T = \left\{\begin{bmatrix}\Delta_u & 0\\ 0 & \Delta_p\end{bmatrix}, \Delta_u\in\Delta^*,\ \Delta_p\in\not\emptyset\right\} \tag{14}$$

where Δ_u and Δ_p (fictitious uncertain block) represent uncertainty and performance requirements, respectively. The closed loop of system for all $\Delta\in\Delta_T$ and $\left\|\Delta\right\|_\infty \le 1$, guarantees the RP if and only if

$$\sup_{w\in R}\ \mu_\Delta\left(M\right) \le 1 \tag{15}$$

According to above theorems, the upper bound for RS and RP are below one at all frequencies, as shown in Fig. 7 and Fig. 8. This means that the RS and RP (for ±90% changes in H and D) are satisfied.

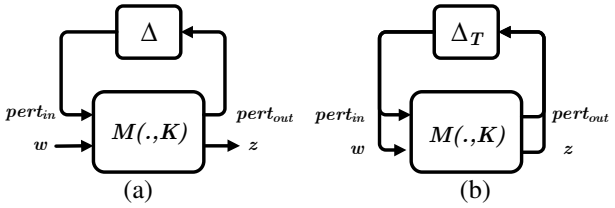

Fig. 6. Standard structure for μ-synthesis: a) robust stability, b) robust performance.

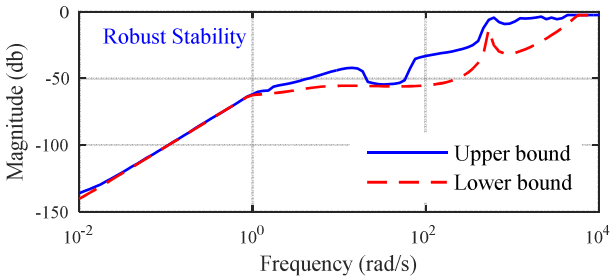

Fig. 7. Robust stability based on μ-synthesis (upper bound of μ must be less than one at all frequencies).

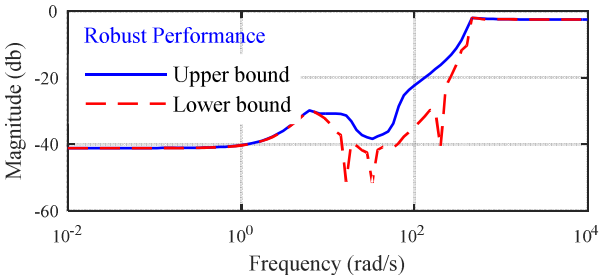

Fig. 8. Robust performance based on μ-synthesis (upper bound of μ must be less than one at all frequencies).

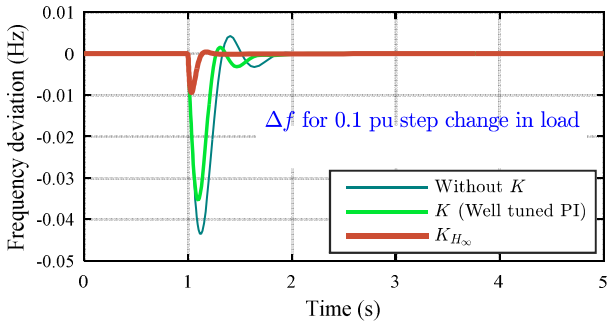

Fig. 9. Frequency deviation of the test MG under 0.1 pu step change in ΔP_L.

The frequency response of the test system for different scenarios i.e., without any controller, with the well-tuned PI controller, and under H_∞ robust controller (K_{H_∞}), is shown in Fig. 9.

V. Robust\Optimal Tuning of Virtual Parameters Based on H_∞ Robust Controller

The flexibility of VSG concept in parameters setting is a great advantage comparing the real SGs. Conventionally, the virtual parameters are defined either using the parameters of conventional SGs or based on trial and error method. In both cases, however, proper tuning of the VSG parameters is not guaranteed. A control method is proposed here for robust and

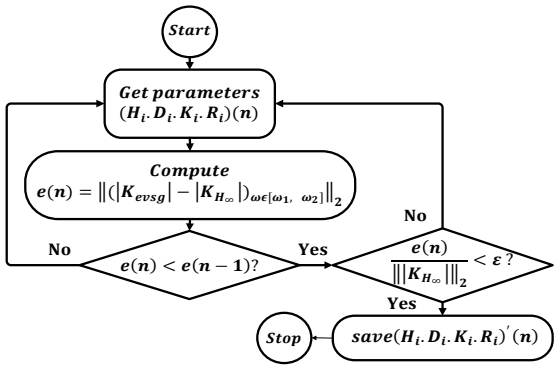

Fig. 10. Proposed algorithm for matching the bode diagram of K_{evsg} and K_{H_∞}.

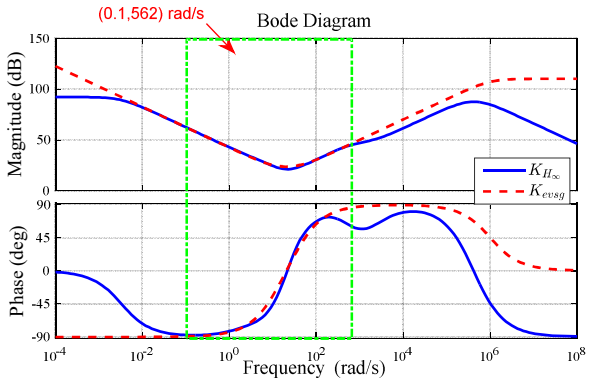

Fig. 11. Comparing Bode diagram of K_{evsg} and K_{H_∞}.

optimal tuning of the parameters of the virtual controller based on the given robust control criterion in Section IV.

A. *Proposed Method*

The basis of this method is to match up the frequency response of virtual controller, K_{evsg}, with the frequency response of designed robust controller, K_{H_∞}. The idea is to have a similar response among tracking the same robust performance index for two controllers in the nominal and operating frequency range. Notice that the structure of virtual controller is much simpler than the designed high order robust controller which is a great advantage.

Once both systems are minimum phase, by matching the magnitude of the systems, phases will be matched automatically. Since K_{H_∞} and K_{evsg} are minimum phase, we try to match the magnitude of two controllers in the operating frequency range. For this aim, a 2-norm concept is used to minimize the difference between the magnitudes of the two controllers in 2-coordination domain as follows.

$$\min_{\omega\in(\omega_1,\omega_2)} e = \left\| |K_{evsg}(\omega)| - |K_{H_\infty}(\omega)| \right\|_2 \qquad (16)$$

To minimize (16), a simple algorithm is introduced as shown in Fig. 10. This algorithm presents a simple numerical search technique among a wide range of possible solutions with given step size and lower and upper limits. It searches for such virtual parameters that makes the normalized *e(n)* smaller than a specified value (ε). As a result, the virtual controller can inherit robustness\optimality of the H_∞ robust controller.

The frequency range of ω is selected according to the

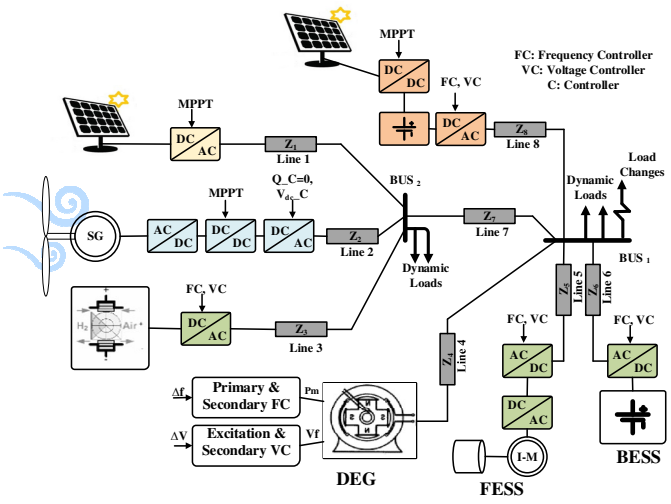

Fig. 12. Details of the MG test system.

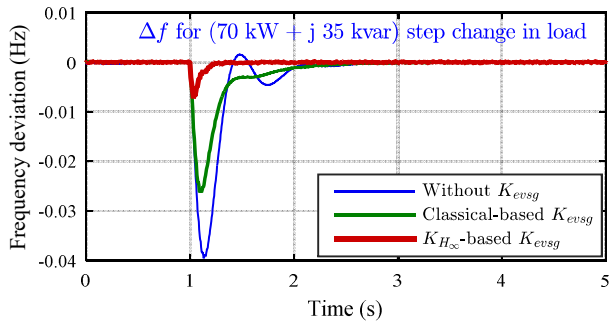

Fig. 13. Frequency response of the system under a step load change for different scenarios.

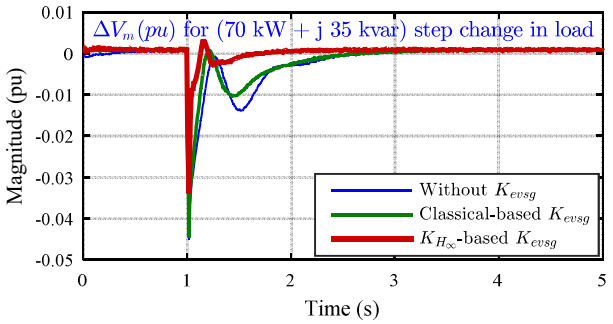

Fig. 14. The amplitude of load bus voltage deviation under a step load change.

suitable and appropriate damping frequency range of Δf, i.e., the range of frequency/speed changes of DG's output power. For $\omega\in(0.1,562)\,rad/s$, and using the proposed method, the optimal virtual parameters are obtained as follow.

$$H_i = 0.9,\quad D_i = 10.4,\quad K_i = 12.9,\quad R_i = 2.8 \qquad (17)$$

Bode diagram of K_{H_∞} and K_{evsg} for the defined parameters are plotted in Fig. 11. As depicted, Bode diagrams of both controllers are well matched in the operating frequency range. Thus, one can conclude that the controllers provide similar performance in the defined frequency range.

Although the EVSG control structure is low-order and too

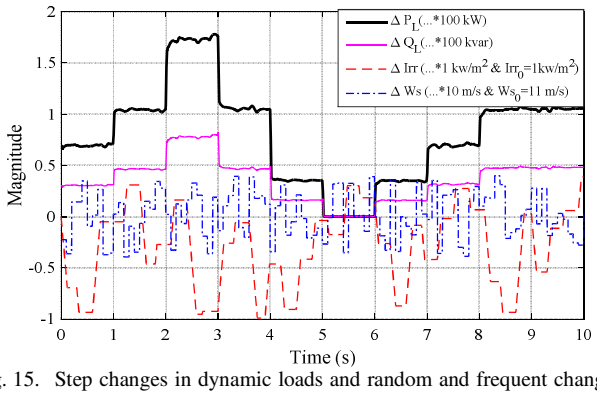

Fig. 15. Step changes in dynamic loads and random and frequent changes in solar irradiance and wind speed.

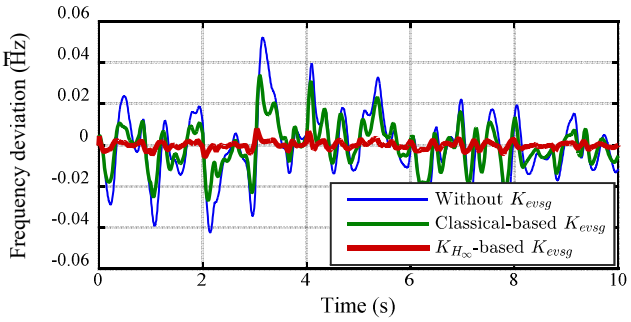

Fig. 16. Frequency variation of the system to the disturbances shown in Fig. 15.

simple, it properly emulates the positive properties of required inertia, damping characteristic, primary and secondary control loops associated with the well-known synchronous generators. Furthermore, it inherits robustness and optimality of the full-dynamics high-order and complex H_∞ robust controller by tracking its robust performance index via the given developed algorithm (Fig. 10). In practice, a computer or at least a microcontroller is needed to implement the H_∞ controller; while the synthesized EVSG can be easily realized using few passive circuit elements. Therefore, from total cost point of view the developed EVSG is much cheaper than its equivalent H_∞ controller.

In the next section, the effectiveness and performance of virtual controller with the defined parameters are investigated.

VI. Time-Domain Simulation Results

The simplified frequency response model of the MG test system in Fig. 3, was used for frequency analysis and designing the virtual controller. To verify the effectiveness of the proposed control method, the MG case study of Fig. 3 is simulated in MATLAB SPS toolbox. The MG case study including DGs, power electronics interfaces, line impedances, loads is shown in Fig. 12. Electrical and control parameters are provided in Table II, Table III, Table IV and Table VI of Appendix. Nominal frequency and voltage of the system are 50 Hz and 380-volt line to line, respectively. The virtual controller is applied to the PV_2 system and rest of components is controlled as already explained. It is worth mentioning that for the given case study, the order of resulted H_∞ robust

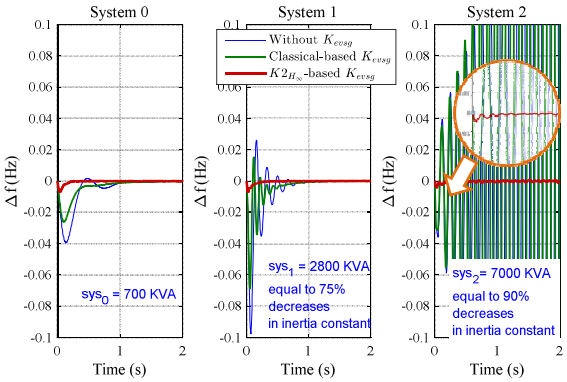

Fig. 17. Frequency deviation of the system 0, system 1 and system 2 under a step load change (evaluating the effectiveness of the proposed controller in presence of system uncertainty).

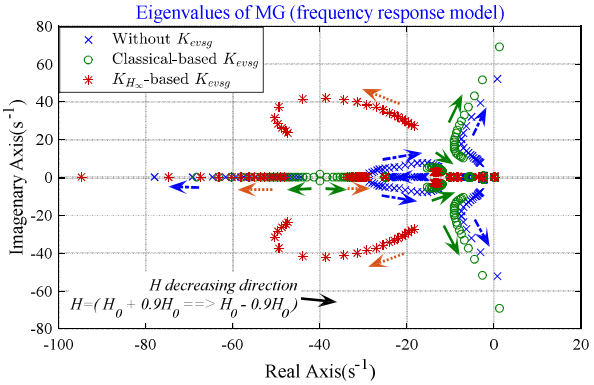

Fig. 18. Trajectory of system's Eigenvalues against decreasing H (±90% changes) for all three controllers.

controller is 22; while the order of EVSG control is always 2, as given in (5).

The following scenarios show the frequency response of the system in the presence of disturbances (ΔP_L, ΔP_W, and ΔP_S) and high perturbation of H and D parameters as uncertainty (equal to the high penetration of none/less inertia DGs). The time-domain simulation results are shown and compared for three cases: 1) without K_{evsg} (blue color), 2) with classical-based K_{evsg} (green color), where virtual parameters are defined using trial and error comparing with the parameters of real SGs, 3) with K_{H_∞}-based K_{evsg} (red color).

Scenario I- Performance assessment under step load change

In the first scenario, the performance of the proposed virtual controllers under step load change is studied. The system's frequency response is shown in Fig. 13, where a desirable performance is observed by the virtual controller comparing the other two cases. The amplitude of load bus voltage is depicted in Fig. 14. As seen from this figure, the controllers have a different effect on voltage regulation. Thus, one can conclude that frequency and voltage responses are not fully decoupled. This correlation mainly depends on the ratio of line resistance and inductances [1]. Therefore the emulation of the kinetic energy of SGs in MGs can affect the voltage response. This is an important issue which may be considered in the future works.

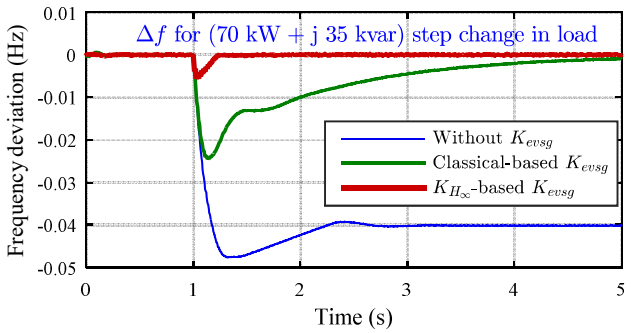

Fig. 19. Performance of the proposed virtual controller considering DEG limitation in reserve energy.

Scenario II- Performance assessment under various disturbances

In this scenario, solar irradiation, wind speed, and dynamic loads change are considered simultaneously (see Fig. 15). For the applied severe step changes in dynamic loads and random and severe changes in solar irradiation and wind speed, the MG's frequency deviation response is shown in Fig. 16. While the traditional controllers do not provide a satisfactory performance, the proposed virtual controller maintains the frequency deviations within an acceptable range around the nominal frequency under the given disturbances.

Scenario III- Performance assessment under system uncertainties

According to (2), when the proportion of none-inertia sources are increased, the system's inertia constant (H_{sys}) will be decreased. How the proposed virtual controller compensates the effects of low inertia of the system, is examined in this section. The following scenarios are considered:

- The size of test system increased up to 2800 kVA by adding non-inertia sources, i.e., 75% decrease in H_{sys} (system 1),
- The size of test system increased up to 7000 kVA by adding more non-inertia sources, i.e., 90% decrease in H_{sys} (system 2).

The nominal power and dynamic loads for the initial system (system 0), system 1 and system 2 are provided in Table III and Table V. The results of this study are illustrated in Fig. 17. This figure shows the frequency responses of the test system against step changes in dynamic loads (0.1 pu in ΔP_L and 0.025 pu in ΔQ_L). It should be noted that the systems are in a steady state before occurring the load change.

While the proposed controller provides a superior performance for all three scenarios, the other two controllers are not able to maintain system stability in the third scenario, i.e. system 2. To study whether these results are matched with the done frequency analysis using the frequency response model (see Fig. 3) in Section III, the trajectory of closed-loop system's effective eigenvalues against changing the inertia constant, H is provided in Fig. 18. While for the other two controllers the eigenvalues of the closed-loop system move toward the right side of s-plane, the complex eigenvalues margin increases in case the proposed virtual controller, i.e., K_{H_∞}-based K_{evsg}, is applied. Indeed, this figure verifies the results obtained from the simulations in Fig. 17.

Scenario IV- Performance assessment considering limits in DG's reserve energy

In the previous scenarios, we assumed all responsible DGs have sufficient reserve energy to support power changes. Here, it is assumed that the DEG does not have enough energy required for frequency regulation. For such a scenario, the frequency response under step load change is depicted in Fig. 19. As seen, the results verify the effectiveness of the proposed method in controlling the system frequency under severe disturbance. The classical–based K_{evsg} provides a slow dynamics, while the K_{H_∞}-based K_{evsg} shows a superior performance with no steady state error.

VII. Conclusion

This paper introduces a new concept called extended virtual synchronous generator to increase the inertia of power electronics-based systems, e.g., microgrids, and accordingly providing frequency support for the grid. Inspired by conventional SGs, the proposed virtual controller includes three virtual modules: rotor, primary control, and secondary control. The virtual parameters are fine-tuned using an H_∞ robust control method. An MG test system is used to validate the effectiveness of the proposed approach. The simulation results and also stability analysis indicate that correlating the virtual controller and robust controller is an effective and suitable approach to the optimal and robust designing of the VSG parameters. The results report superior performance of the proposed robust virtual controller in the presence of high-uncertainty situation and severe disturbances.

Appendix

Here, electrical and control parameters of the MG test system shown in Fig. 12 are given.

TABLE II
DG's Nominal Power (NP), Initial Active/Reactive Power, and Frequency\Voltage Controller (F\V.C) Applied to the DGs

DG	DEG	WT	PV_1	PV_2	FC	BESS	FESS
NP (kVA)	200	100	30	200	70	45	45
P0 (kW)	130	105, MPPT	30, MPPT	40	50	35	35
Q0 (kVAR)	40	-	-	20	35	22.5	22.5
F.C	R_p=3, PI	-	-	K_{evsg}	R_p=1	R_p=1	R_p=1
V.C	PI	-	-	R_q=1	R_q=1	R_q=1	R_q=1

TABLE III
MG Dynamic Loads for Different System

Dynamic loads	BUS_2	BUS_2	BUS_1	BUS_1	BUS_1
SYSTEM 0					
P (kW)	50	135	70	40	130
Ql (kVAR)	5	10	10	30	45
Qc (- kVAR)	1	2	2	10	5
SYSTEM 1					
P (kW)	220	535	600	120	130
Ql (kVAR)	50	20	100	50	45
Qc (- kVAR)	8	2	10	10	5
SYSTEM 2					
P (kW)	220	2800	600	2600	130
Ql (kVAR)	50	100	100	300	45
Qc (- kVAR)	8	20	10	10	5

TABLE IV
MG LINES IMPEDANCE

Line	1	2	3	4	5	6	7	8
R (Ω)	0.1	0.3	0.4	0.25	0.2	0.2	0.33	0.33
L (mH)	0.4	1	1.2	0.6	0.5	0.5	1.1	1.1

TABLE V
DG'S NOMINAL POWER (NP), INITIAL ACTIVE/REACTIVE POWER IN SYSTEM 1AND SYSTEM 2

DG	DEG	WT	PV_1	PV_2	FC	BESS	FESS
SYSTEM 1							
NP (kVA)	200	100	600	600	350	450	450
P0 (kW)	130	105, MPPT	600, MPPT	120	250	350	350
Q0 (kVAR)	40	-	-	60	90	70	70
SYSTEM 2							
NP (kVA)	200	2200	2800	600	350	450	450
P0 (kW)	130	2200, MPPT	2800, MPPT	120	250	350	350
Q0 (kVAR)	40	-	-	60	90	70	70

TABLE VI
SOME COMMON DG'S PARAMETERS RANGE

Parameter	Value
Current control (PI)	K_p = 0.2-2, K_i = 350-500
Switching frequency	2-12 kHz
LCL filter	L_1=0.3-0.6 (pu), C=400-3000 (var), L_2=0.15-0.3 (pu)
MPTT algorithm	Perturb and observe

REFERENCES

[1] H. Bevrani, B. Francois, and T. Ise, *Microgrid Dynamics and Control*, NJ, USA: Wiley, July 2017.

[2] J. M. Guerrero, J. C. Vasquez, J. Matas, L. G. de Vicuña, and M. Castilla, "Hierarchical control of droop-controlled AC and DC microgrids—A general approach toward standardization", *IEEE Trans. Ind. Electron.*, vol. 58, no. 1, pp. 158–172, Jan. 2011.

[3] H. Bevrani, *Robust Power System Frequency Control*, 2nd edition, Gewerbestrasse, Switzerland: Springer, 2014.

[4] H. Bevrani, M. Watanabe, and Y. Mitani, *Power System Monitoring and Control*. Hoboken, NJ, USA: IEEE-Wiley, Jun. 2014.

[5] H. Bevrani, M. Feizi and S. Ataee, "Robust Frequency Control in an Islanded Microgrid: Hinf and μ-Synthesis Approaches", *IEEE Trans. Smart Grid,* vol. 7, no. 2, pp. 706–717, July 2015.

[6] Y. Han, P. M. Young, A. Jain, and D. Zimmerle, "Robust control for microgrid frequency deviation reduction with attached storage system", *IEEE Trans. Smart Grid*, vol. 6, no. 2, pp. 557–565, Mar. 2015.

[7] V. P. Singh, S. R. Mohanty, N. Kishor, and P. K. Ray, "Robust *H*-infinity load frequency control in hybrid distributed generation system", *Int. J. Elect. Power Energy Syst.*, vol. 46, pp. 294–305, Mar. 2013.

[8] S. Yang, Q. Lei, F. Z. Peng, and Z. Qian, "A robust control scheme for grid-connected voltage-source inverters", *IEEE Trans. Ind. Electron*., vol. 58, no. 1, pp. 202–212, Jan. 2011.

[9] M. Dreidy, H. Mokhlis, and S. Mekhilef, "Inertia response and frequency control techniques for renewable energy sources: A review", *Renewable and Sustainable Energy Reviews*, vol. 69, pp. 144–155, Mar. 2017.

[10] Y. Hirase, K. Abe, K. Sugimoto, and Y. Shindo, "A grid connected inverter with virtual synchronous generator model of algebraic type", *IEEJ Trans. Power Energy*, vol. 132, no. 4, pp. 371–380, Jan. 2012.

[11] Y. Hirase, K. Abe, K. Sugimoto, K. Sakimoto, H. Bevrani, and T. Ise, "A novel control approach for virtual synchronous generators to suppress frequency and voltage fluctuations in microgrids", *Applied Energy*. In Press, 2017.

[12] H. Bevrani, T. Ise, and Y. Miura, "Virtual synchronous generators: A survey and new perspectives", *Int. J. Elect. Power Energy Syst.*, vol. 54, no. 1, pp. 244–254, Jan. 2014.

[13] I. Cvetkovic, D. Boroyevich, R. Burgos, Chi Li, M. Jaksic and P. Mattavelli, "Modeling of a virtual synchronous machine-based grid-interface converter for renewable energy systems integration", in Proc. IEEE 15th Workshop on Control and Modeling for Power Electron. (COMPEL), Santander, 2014, pp. 1-7.

[14] H. Wu, X. Ruan, D. Yang, X. Chen, W. Zhao, Z. Lv and Q. Zhong, "Small-Signal Modeling and Parameters Design for Virtual Synchronous Generators", *IEEE Trans. Ind. Electron.*, vol. 63, no. 6, pp. 4292–4303, Mar. 2016.

[15] D. Li, Q. Zhu, S. Lin and X. Y. Bian, "A Self-Adaptive Inertia and Damping Combination Control of VSG to Support Frequency Stability", *IEEE Trans. Energy Convers.*, vol. 32, no. 1, pp. 397-398, Mar. 2017.

[16] L. Y. Lu and C. C. Chu, "Consensus-Based Secondary Frequency and Voltage Droop Control of Virtual Synchronous Generators for Isolated AC Micro-Grids," *IEEE J. Emerg. Sel. Topics in Circuits and Sys.*, vol. 5, no. 3, pp. 443-455, Sep. 2015.

[17] B. Rathore, S. Chakrabarti and S. Anand, "Frequency response improvement in microgrid using optimized VSG control", in Proc. *Nat. Power Sys. Conf. (NPSC)*, Bhubaneswar, 2016, pp. 1-6.

[18] T. Shintai, Y. Miura and T. Ise, "Oscillation Damping of a Distributed Generator Using a Virtual Synchronous Generator", *IEEE Trans. Power Del*, vol. 29, no. 2, pp. 668-676, Apr. 2014.

[19] J. Liu, Y. Miura and T. Ise, "Comparison of Dynamic Characteristics Between Virtual Synchronous Generator and Droop Control in Inverter-Based Distributed Generators", *IEEE Trans. Power Electron.*, vol. 31, no. 5, pp. 3600-3611, May 2016.

[20] Y. Hu, W. Wei, Y. Peng and J. Lei, "Fuzzy virtual inertia control for virtual synchronous generator", in Proc. *35th Chinese Control Conf. (CCC)*, Chengdu, 2016, pp. 8523-8527.

[21] P. Kundur, *Power system stability and control*, McGraw-Hill, 1994.

[22] M. H. Rashid, *Power Electronics Handbook*, 2nd edition, New York, Academic, 2007.

[23] F. Lin Luo, H. Ye, M. H. Rashid, *Digital Power Electronics and Applications*, San Diego, California, USA Elsevier, 2005.

[24] J. Rocabert, A. Luna, F. Blaabjerg, and I. Paper, "Control of Power Converters in AC Microgrids," *IEEE Trans. Power Electron.*, vol. 27, no. 11, pp. 4734–4749, Nov. 2012.

[25] M. C. Chandorkar, D. M. Divan, and R. Adapa, "Control of parallel connected inverters in standalone ac supply systems," *IEEE Trans. Ind. Appl.*, vol. 29, no. 1, pp. 136–143, Jan./Feb. 1993.

[26] H. Bevrani, F. Habibi, P. Babahajyani, M. Watanabe and Y. Mitani, "Intelligent Frequency Control in an AC Microgrid: Online PSO-Based Fuzzy Tuning Approach", *IEEE Trans. Smart Grid*, vol. 3, no. 4, pp. 1935-1944, Dec. 2012.

[27] K. Zhou, *Essentials of Robust Control*, Prentice Hall, 1999.

[28] R. H. Lasseter, "Smart Distribution: Coupled Microgrids," *Proceedings of the IEEE,* vol. 99, pp. 1074-1082, June 2011.